Vol. No.6, Issue No. 06, June 2017 www.ijarse.com



Cavity Model Based Analysis of Gunn Loaded Annular Ring Microstrip Patch Antenna

Arvind Mishra¹, Km Pankaj², B P Singh³

¹Department of Physics, G L Bajaj Institute of Technology and Management, Greater Noida, (India)

ABSTRACT

The present work describes the cavity model based analysis of Gunn diode loaded annular ring microstrip patch antenna at 8.2 GHz. To optimize the antenna characteristics, a study has been carried out on the different parameters of the antenna as a function of Gunn diode bias voltage and threshold voltage. It is concluded that the tuning range is higher at higher V_{Th} (7.7%) and lower at lower values of V_{Th} (5.1%) for a given range of bias voltage. In this study it has also been found that the value of reflection coefficient is lowest (-0.020) at 8.245 GHz which is the design frequency of the active patch.

Keywords: Microstrip Antenna; Annular Ring Patch; Gunn Diode; Radiation Pattern; Mismatch Loss.

I. INTRODUCTION

The active-integrated microstrip antenna has become prominent now-a-day in the field of microwave and millimeter wave communications as it offers advantages of enhanced power capability, improved bandwidth, gain, beam-width, low profile, light weight, easy fabrication and electronic tenability [1-3]. The major drawback of the microstrip antennas is very narrow bandwidth. However, the annular ring microstrip antenna provides larger bandwidth controlled by the ratio of outer o inner radii. Several interesting properties are associated with annular ring antennas and these interesting features attracted the attention of several active antenna investigators [4].

The present work describes the equivalent circuit modeling based analysis of Gunn diode loaded annular ring microstrip patch antenna at 8.2GHz. Consequently, various parameters such as reflection coefficient, mismatch loss, quality factor, band width and radiation pattern of the antenna are evaluated as a function of bias voltage at a particular threshold value and the results thus obtained are also compared with patch alone.

II. THEORETICAL CONSIDERATIONS

The structure of the antenna integrated with Gunn-diode is shown in Fig 1. The Gunn-integrated annular ring microstrip antenna with its equivalent circuit in terms of parallel combination of an inductance L, a capacitance C, and admittance Y is shown in Fig 2. The values of LCR can be given as [5]

$$L = \frac{\mu h}{\pi k_*^2 [n,m]} [J_n(K_1 c) Y_n'(K_1 a_s) - Y_n(K_1 c) J_n'(K_1 a_s)]^2$$
(1)

$$R = R_{\varepsilon}[Y] \tag{2}$$

²Department of Physics, Noida Institute of Engineering and Technology, Greater Noida, (India)

³Department of Physics, Institute of Basic Sciences, Dr B R Ambedekar University, Agra,(India)

Vol. No.6, Issue No. 06, June 2017

www.ijarse.com



$$C = \frac{\mu \varepsilon_0 \varepsilon_\gamma}{LK_s^2} \tag{3}$$

where

$$\begin{split} &[n,m] = \frac{1}{2K_1^2} [(K_1^2 b_e^2 - 1) \{J_n(K_1 b_e) Y_n'(K_1 a_e) - Y_n(K_1 b_e) J_n'(K_1 a_e)\}^2 \cdot \frac{1}{\pi^2 K_1^2 a_e} (K_1^2 a_e^2 - 1)] \\ &R_e[Y] = R_e \left[\frac{\pi}{h} \Big\{ (\frac{E_{nm}(a,\phi)}{E_{nm}(c,\phi)})^2 g(a,a) + \left(\frac{E_{nm}(b,\phi)}{E_{nm}(c,\phi)}\right)^2 g(b,b) - \frac{2E_{nm}(a,\phi)E_{nm}(b,\phi)}{E_{nm}^2(c,\phi)} y(a,b) \Big\} \right] \\ &E_{nm}(\rho,\phi) = z \{J_n(k_1 b_e) Y_n'(k_1 a_e) - Y_n(k_1 b_e) J_n'(k_1 a_e)\} \end{split}$$

Also y(a, b) is the mutual admittance between apertures, g (a, a) is the edge conductance at inner radius and g (b, b) is the edge conductance at outer radius. The values of mutual admittance between the apertures at $\rho = a$ and $\rho = b$ is given by [6]

$$y(a,b) = \frac{jabh}{2\pi^{2}\mu\omega} \int_{0}^{2\pi} \cos\phi \left[\int_{0}^{2\pi} \cos\alpha \frac{e^{-jk_{0}r_{1}}}{r_{1}^{3}} \left\{ 2\cos(\phi - \alpha)(1 + jk_{0}r_{1}) + \frac{(b\cos(\phi - \alpha) - a)(b - a\cos(\phi - \alpha))}{r_{1}^{2}(k_{0}^{2}r_{1}^{2} - 3jk_{0}r_{1} - 3)} \right\} d\alpha \right] d\phi$$
(4)

The values of edge conductances g(a, a) and g(b, b) obtained by substituting b = a and a = b respectively in above equations and retaining the real part only. Here a and b be the inner and outer radius of annular ring microstrip antenna respectively, μ be the permeability of the substrate, b be the thickness of dielectric substrate, b be the resonant wave number, b be the relative permittivity of the substrate and b be the effective permittivity of the substrate.

The effective inner and outer radius of the annular ring microstrip antenna can be written as [7]

$$a_{\varepsilon} = a \left(1 - \frac{2hX_{d}}{a\pi\varepsilon_{u}} \right) \tag{5}$$

And

$$b_s = b\left(1 + \frac{2hX_b}{b\pi s_r}\right) \tag{6}$$

where X_a is given by

$$x_a = \ln\left(\frac{b}{2b}\right) + 1.41\varepsilon_r + 1.77 + \frac{h}{b}(0.268\varepsilon_r + 1.65) \tag{7}$$

The expression for X_b is obtained by replacing the radius 'a' with 'b' in equation (7). The design parameters of the ring microstrip patch antenna for the active device at non-woven glass-PTFE substrate ($\epsilon_r = 2.32$, Tan $\delta = 0.0012$) of thickness 1.59 mm with operating frequency 8.2 GHz are given in Table 1. The equivalent circuit of annular ring microstrip antenna and Gunn diode are given in Fig 2. The admittance Y of annular ring microstrip antenna is expressed as [8]

$$Y = G + jB = \frac{1}{R} + j\omega C + \frac{1}{j\omega C}$$

where G and B are the real and imaginary parts of admittance Y. Thus

$$Y = \frac{1 + j\omega L - \omega^2 LC}{j\omega LR} \tag{8}$$







Now the input impedance (Zin) of annular ring microstrip antenna

$$Z_{in} = \frac{1}{Y} = \frac{R\omega^2 L^2 - jR^2 \omega L (1 - \omega^2 LC)}{R^2 (1 - \omega^2 LC) + \omega^2 L^2}$$
(9)

Separating for real and imaginary parts of the impedance of annular ring microstrip antenna as

$$R_{s}Z_{in} = \frac{R\omega^{2}L^{2}}{R^{2}\omega^{2}L^{2} + (1 - \omega^{2}LC)^{2}}$$
(10)

$$I_m Z_{in} = R^2 \omega L (1 - \omega^2 LC) / R^2 (1 - \omega^2 LC)^2 + \omega^2 L^2$$
(11)

The impedance of Gunn-loaded ARMSA can be obtained as

$$Z = \frac{(R_{d} - R)\omega^{2}L^{2}RR_{d} + j\omega L(1 - \omega^{2}LC)R^{2}R_{d}^{2}}{R^{2}(1 - \omega^{2}LC)^{2} + \omega^{2}L^{2}}$$
(12)

Separating for real and imaginary parts of the impedance of Gunn-loaded ARMSA as

$$R_{e}Z = \frac{(R_{d} - R)\omega^{2}L^{2}RR_{d}}{R^{2}(1 - \omega^{2}LC)^{2} + \omega^{2}L^{2}}$$
(13)

$$I_{m}Z = \frac{(1 - \omega^{2}LC)R^{2}R_{d}^{2}\omega L}{R^{2}(1 - \omega^{2}LC)^{2} + \omega^{2}L^{2}}$$
(14)

To obtain the effective resonance frequency of the active patch, the imaginary part of the input impedance is equated to zero, which gives

$$\omega_{\rm r} = \frac{1}{\sqrt{LC}}$$

or

$$f_{r} = \frac{\omega_{r}}{2\pi} = \frac{1}{2\pi} \sqrt{\frac{1}{LC}}$$
 (15)

In Gunn-oscillator circuit when terminal voltage is below the threshold voltage, the diode is ohmic with relatively small parallel capacitance and the current is exponentially limited by L/R_0 time constant. The resonant frequency of the active patch is given by [9]

$$f_{r} = \frac{1}{T} = \frac{1}{\frac{L}{R_{d}(V_{b}/V_{th})} + 2\pi\sqrt{LC}}$$
 (16)

The quality factor of resonant ARMSA is given by [10]

$$Q' = \omega_0 RC = \frac{R}{\omega_0 L}$$
 (17)

while the quality factor of Gunn loaded ARMS is found as

$$\frac{1}{Q_{L}} = \frac{1}{Q_{e}} + \frac{1}{Q'} \tag{18}$$

where Q_{e} is the external quality factor written as $\mid R_{\text{d}} \mid / \omega_0 L$ and

$$R = \frac{|R||R_d|}{(|R|+|R_d|)}$$

Vol. No.6, Issue No. 06, June 2017

www.ijarse.com



The radiation pattern for ARMSA and Gunn loaded ARMSA can be calculated as [11]

$$E_{\theta} = \frac{j^{n} 2hK_{0}E_{0}e^{-jK_{0}r}}{\pi K_{1}r} \left[J_{n}(K_{0}a\sin\theta) - J_{n}(K_{0}b\sin\theta) \frac{J_{n}(K_{1}a)}{J_{n}(K_{1}b)} \right]$$
(19)

$$E_{\phi} = \frac{j^{n} 2nhE_{0}}{\pi K_{1}} \frac{e^{-jK_{0}r}}{r} \frac{\cos\theta \sin\phi}{\sin\theta} \left[\frac{J_{n}(K_{0}a\sin\theta)}{a} - \frac{J_{n}(K_{0}b\sin\theta)}{b} \frac{J_{n}(K_{1}a)}{J_{n}(K_{1}b)} \right]$$
(20)

where $E_0 = hv_0$ and k_0 is given by

$$k_0 = 2\pi/\lambda_0 \tag{27}$$

On the basis of analysis and formulations given above, we have observed the variations between various parameters like resonant frequency, reflection coefficient, mismatch loss, quality factor etc. with bias voltage. In order to compare the performance of the Gunn-active microstrip antenna with unloaded patch alone, calculation were also made for these parameters. The calculated values of relative power values at different angles and different biasing voltage for Gunn loaded patch and patch only are calculated and given in Table III.

III. DESIGN DETAILS

The IMPATT-diode loaded rectangular microstrip antenna is designed using various parameters of rectangular microstrip antenna and IMATT-diode, the details of which are given in Tables 1 and 2.

IV. DISCUSSION OF RESULTS

From the Fig 3 and 4, it is clear that the operating frequency decreases with bias voltage for all values of threshold voltages. However, the antenna operates at higher frequency range at higher value of threshold voltages and lower frequency range at lower values of bias voltages. It is further observed that the frequency increases with threshold voltage. It may be added that the tuning range is higher at higher V_{Th} (7.7%) and lower at lower values of V_{Th} (5.1%) for a given range of bias voltage. Thus the study reveals that the Gunn-loaded ARMSA shows the electronic tunability, which can be adjusted not only by varying the bias voltage but also by varying the threshold voltage. The tuning range of the proposed active antenna shows higher value (6%) at lower bias voltage (8V) and the lower tuning range (3.4%) at higher bias voltage for the entire range of threshold voltage (Fig. 5). From Fig.6 it is clear that the reflection coefficient for the loaded patch is around -0.0306, showing that the antenna can be operated without any significant power loss for the entire range of operation (8.245 - 8.300 GHz). The value of reflection coefficient is lowest (-0.020) at 8.245 GHz which is the design frequency of the active patch. These results are further justified by the lower mismatch at the feed (Fig.7).

In order to compare the Gunn-loaded annular ring microstrip antenna with annular ring microstrip patch only, calculations were made for various parameters such reflection coefficient, mismatch loss, quality factor, radiation pattern and % band-width. The variation of percentage band-width with resonance frequency is shown in Fig. 8. The increment of % band-width of loaded patch over unloaded patch is around 3.17%. Typically the band-width of Gunn loaded ARMSA is 11.07 % as reported earlier. These results are attributed from the quality factor variation with resonant frequency shown in Fig, 9. The radiation patterns for Gunn-loaded ARMSA and ARMSA only are shown in Fig 10. It is observed that the Gunn loaded patch radiates enhanced power as compared to ARMSA only. The radiated power of loaded patch increases with decrease of bias voltage for a particular value of

Vol. No.6, Issue No. 06, June 2017

www.ijarse.com



threshold voltage. It may be concluded the integration of active device to the patch not only provides electronic tunability of frequency but also the power tunability. Thus the radiated power can be adjusted by controlling the bias voltage.

REFERENCES

- [1] Isha Singh and Alka Verma, Analysis of Frequency Agility of Gunn Loaded Circular Microstrip Antenna, MIT International Journal of Electrical and Instrumentation Engineering, Vol. 6(1), 2016
- [2] Neha Gupta, Ramanjeet Singh, An Annular-Ring Microstrip Patch Antenna for Multiband Applications, International Journal of Engineering Research & Technology, Vol. 4(03), 2015
- [3] Sanghamitra Dasgupta and Bhaskar Gupta, Study and Analysis of GUNN Loaded Active Microstrip Patch Antenna, *PIERS Proceedings*, *Vol. 30*, Kuala Lumpur, MALAYSIA, 2012
- [4] B K Kanaujia and B R Vishvakarma, Some investigations on annular ring microstrip antenna, *Indian Journal of Radio and Space physics*, Vol. 32, 2003
- [5] A K Bhattacharyya and R Garg, Arch. Elek. Ubert, Vol. 185(39), 1985
- [6] A K Bhattacharyya and R Garg, Proc. Inst. Elec. Eng, Vol.131, 1984
- [7] I J Bahal and P Bhartia, Microstrip antennas (Artech House, Dedham, Mass., 1980)
- [8] B K Kanaujia and B R Vishvakarma, IEEE Transactions on Antennas and Propagation, Vol.52(1), 2004
- [9] G S Globson, *The Gunn Effect* (Oxford, UK Clarendon, 1974)
- [10] D M Pozar, Microwave Engineering (Wiley, 1998)
- [11] K E Lee and J SDahele, Ann. Des. Telecomm., Vol. 4,1985

Table-ITypical parameters of annular ring microstrip antenna (ARMSA) [8]

Substrate material used	RT Duroid 5870
Relative permittivity of substrate (ε_r)	2.32
Effective relative permittivity (ϵ_r)	2.07
Thickness of dielectric substrate (h)	1.59 mm
The inner radius of annular ring (a)	1 cm
Effective inner radius of annular ring (a _e)	0.84517 cm
The outer radius of annular ring (b)	2 cm
Effective outer radius of annular ring (b _e)	2.14852 cm
Design frequency (f _r)	8.2 GHz
Resistance (R)	39.5095 ohms
Inductance (L)	6.0958 x 10 ⁻¹¹ H
Capacitance (C)	6.199 pF

Vol. No.6, Issue No. 06, June 2017 www.ijarse.com



Table-IITypical parameters of Gunn diode [9]

Туре	MACOM 49104, GaAs
DC resistance	8 ohms
Threshold Voltage (V _{Th})	(2.9 – 4.4)Volts
Operating point I ₀ at V _b mA/Volts	200 at 9 Volts
Oscillating frequency (X-band)	(8 – 12.4) GHz
Operating mode	LSAR mode
Output power mW (725 cw)	(10 – 25) mW at 10 GHz
Conversion Efficiency	(2-5) %
Device Capacitance	0.10 pF
Packing Capacitance	0.27 pF
Series Inductance	0.3 nH
R _{0LC} (K ohm Watt ⁻¹)	25
Packing Type	Pill with cap
Low field resistance (- R _d)	-13.97 Ω
Device negative resistance	-200 Ω
DC bias voltage	(8 – 15) Volts
Device length (L)	70 μm
Diffusion coefficient (D)	207 cm ² sec ⁻¹
Mobility (μ)	8500 cm ² V ⁻¹ sec ⁻¹
Energy band gap (ΔE)	0.31 eV
Density of state ratio (R)	94

Table-III

Calculated Values of Relative Power (dB)

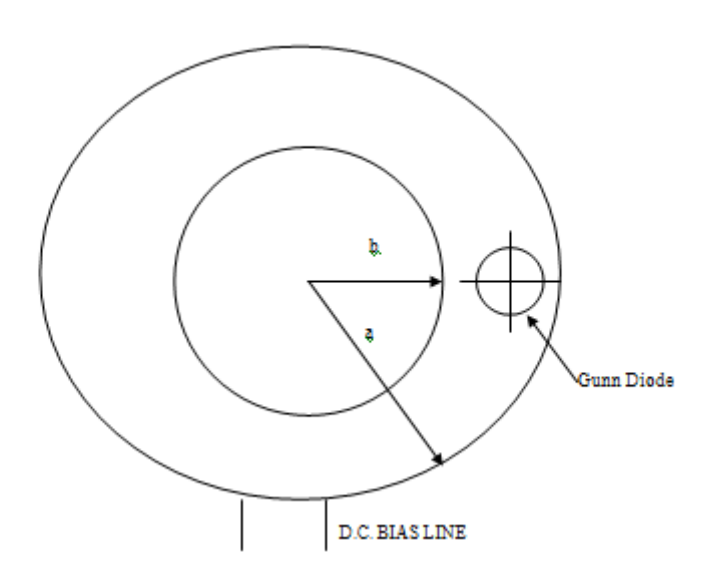
	Relative Power (dB)				
Angle (in degree)	Gunn Loaded Patch (a)				
	8 V	10 V	12 V	15 V	Un Loaded (b)
-80	-23.75	-23.75	-23.75	-23.75	-20.625
-70	-17.5	-19.37	-18.75	-18.85	-17.5
-60	-19.375	-18.75	-18.125	-18.13	-14.37
-50	-36.875	-29.37	-26.875	-24.375	-20.625
-40	-16.875	-19.37	-18.75	-21.875	-31.875
-30	-8.125	-9.37	-15	-11.875	-13.125
-20	-3.125	-3.75	-4.375	-5.625	-8.125

Vol. No.6, Issue No. 06, June 2017

www.ijarse.com



-10	-0.625	-1.25	-1.875	-3.125	-5
0	0	-0.625	-1.25	-1.875	-3.125
10	-0.625	-1.25	-1.875	-3.125	-5
20	-3.125	-3.75	-4.375	-5.625	-8.125
30	-8.125	-9.37	-15	-11.875	-13.125
40	-16.875	-19.37	-18.75	-21.875	-31.875
50	-36.875	-29.37	-26.875	-24.375	-20.625
60	-19.375	-18.75	-18.125	-18.13	-14.37
70	-17.5	-19.37	-18.75	-18.8	-17.5
80	-23.75	-23.75	-23.75	-23.75	-20.625



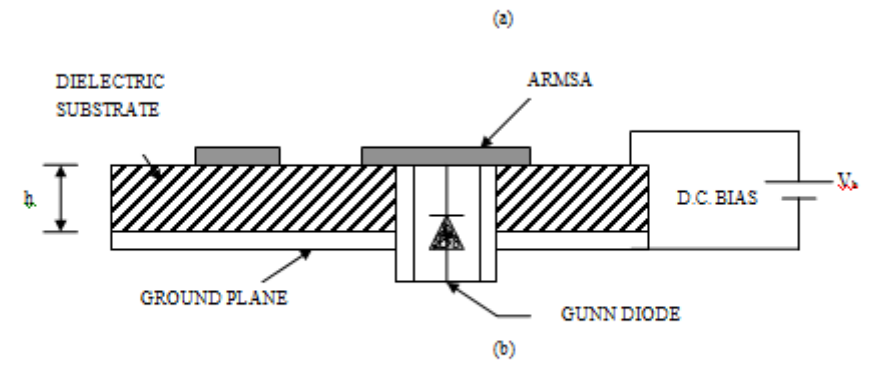


Figure 1: (a) Top view of Gunn integrated ARMSA

(b) Side view of Gunn integrated ARMSA.

Vol. No.6, Issue No. 06, June 2017 www.ijarse.com



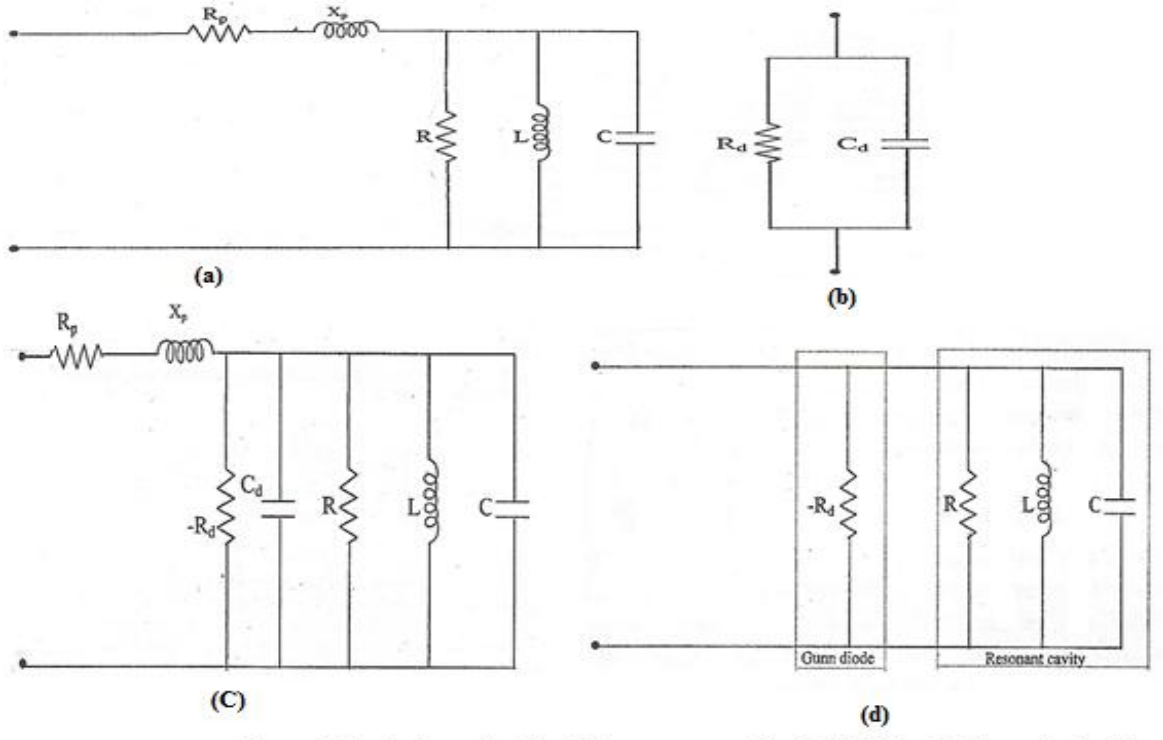


Figure 2: Equivalent circuit of (a) resonant cavity of ARMSA, (b) Gunn diode (c) combined circuit of ARMSA with Gunn diode, (d) simplified circuit for Gunn diode loaded ARMSA

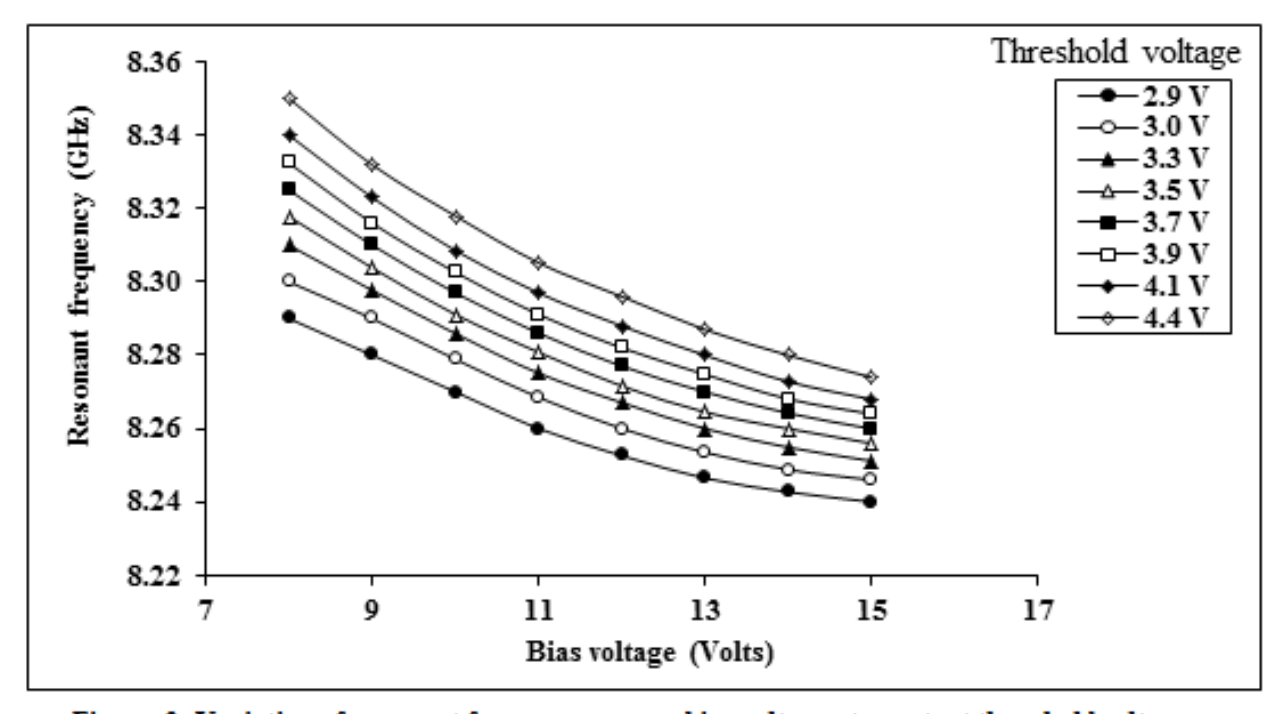


Figure 3: Variation of resonant frequency versus bias voltage at constant threshold voltage.



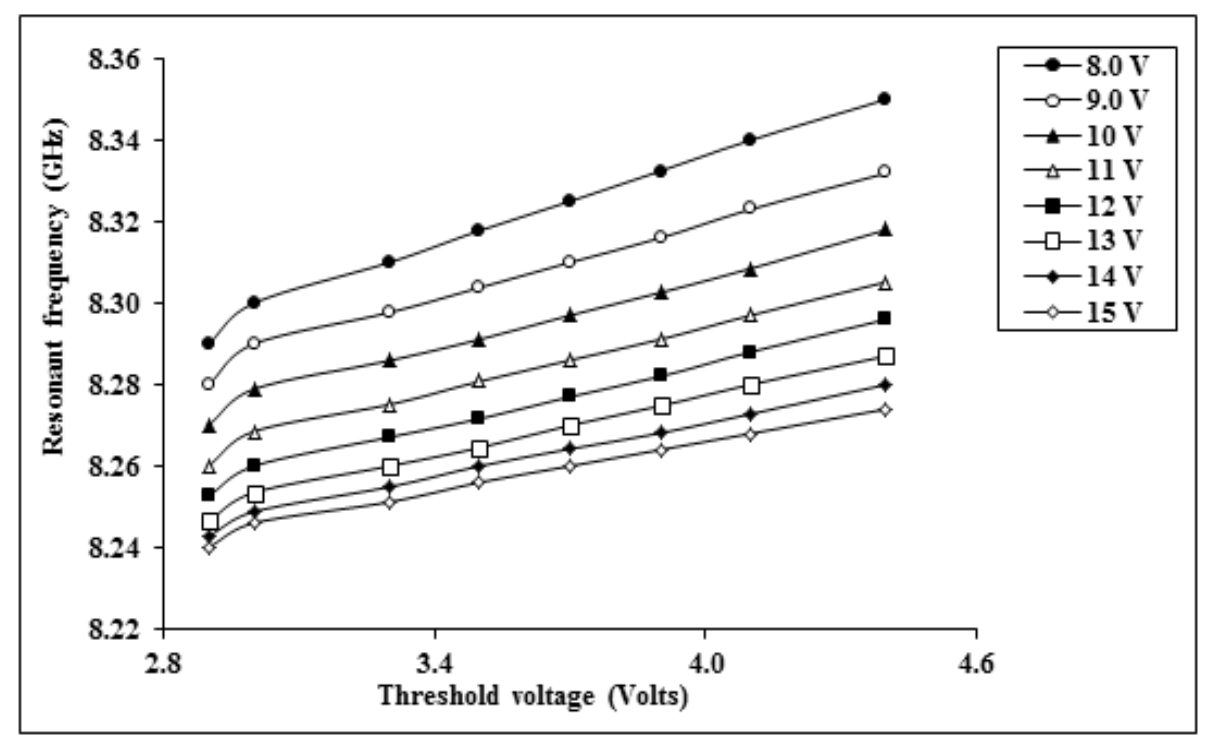


Figure 4: Variation of resonant frequency versus threshold voltage at constant bias voltage.

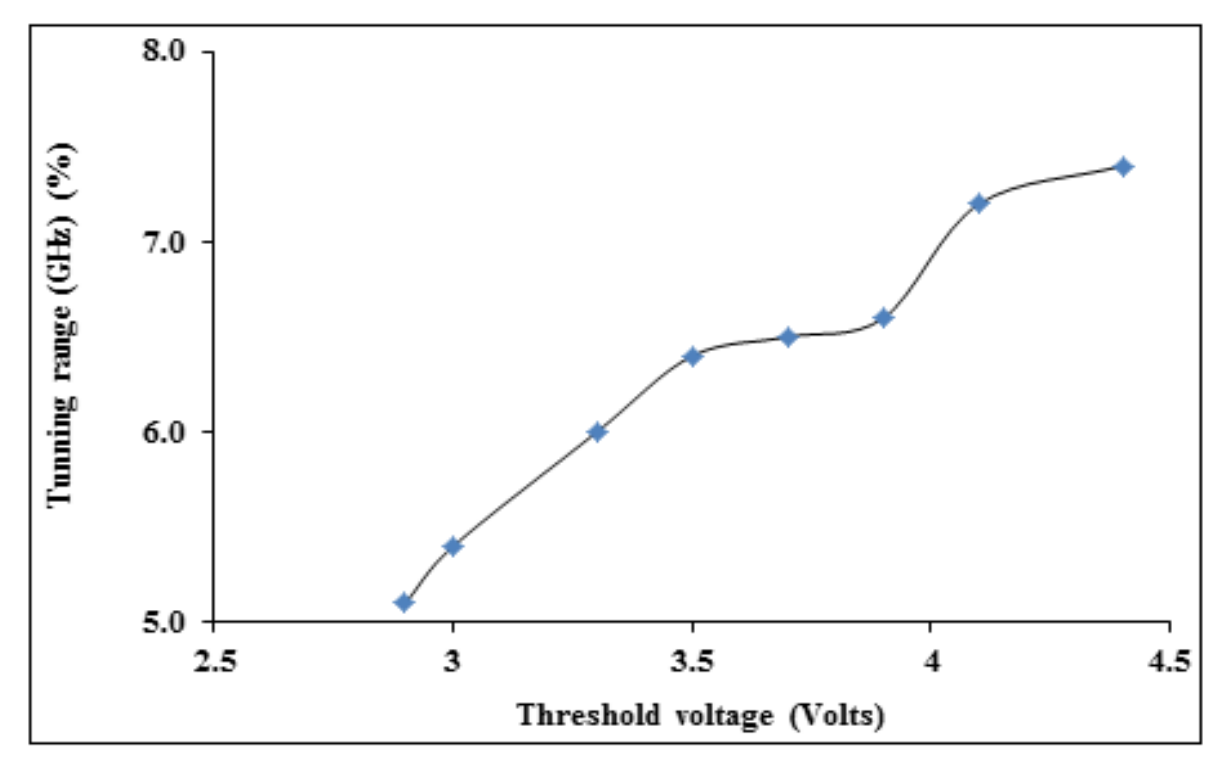


Figure 5: Variation of tuning range with threshold voltage

Vol. No.6, Issue No. 06, June 2017 www.ijarse.com



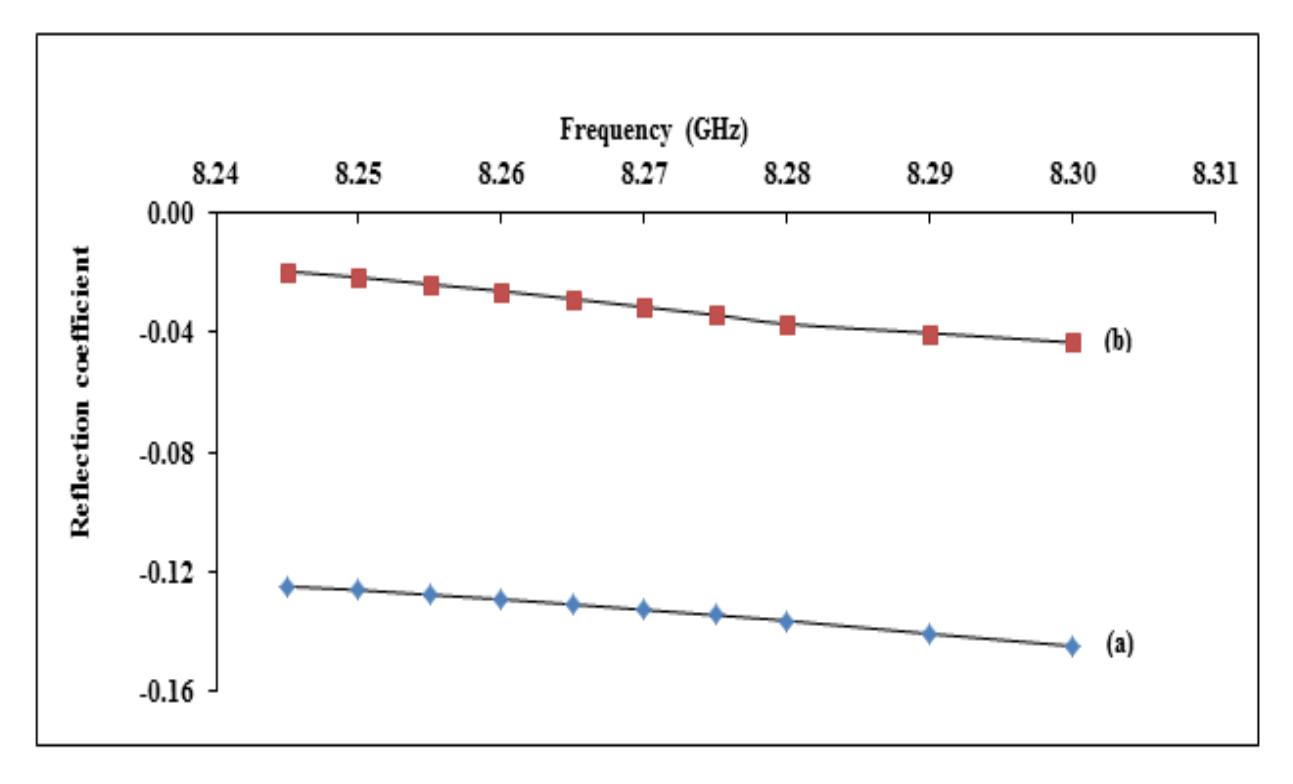


Figure 6: Variation of reflection coefficient with resonant frequency for (a) unloaded and (b) Gunn loaded ARMSA at a constant threshold voltage of 2.9 V.

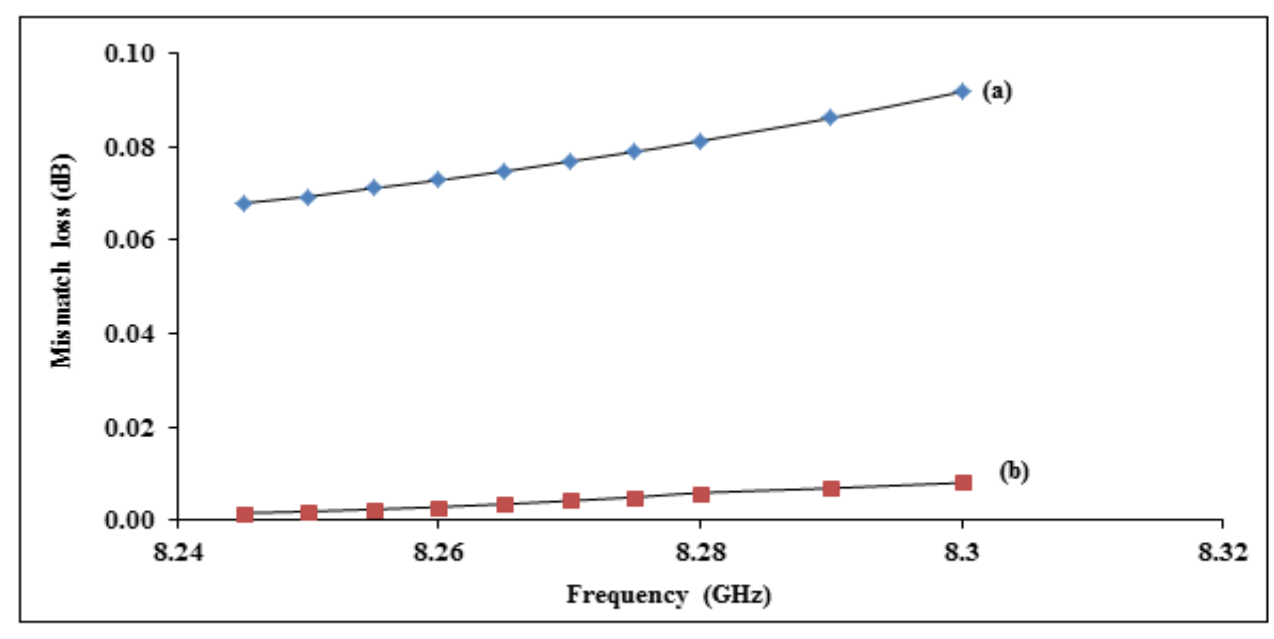


Figure 7: Variation of mismatch loss with resonant frequency for (a) unloaded and (b) Gunn loaded ARMSA at a constant threshold voltage of 2.9 V.

Vol. No.6, Issue No. 06, June 2017 www.ijarse.com



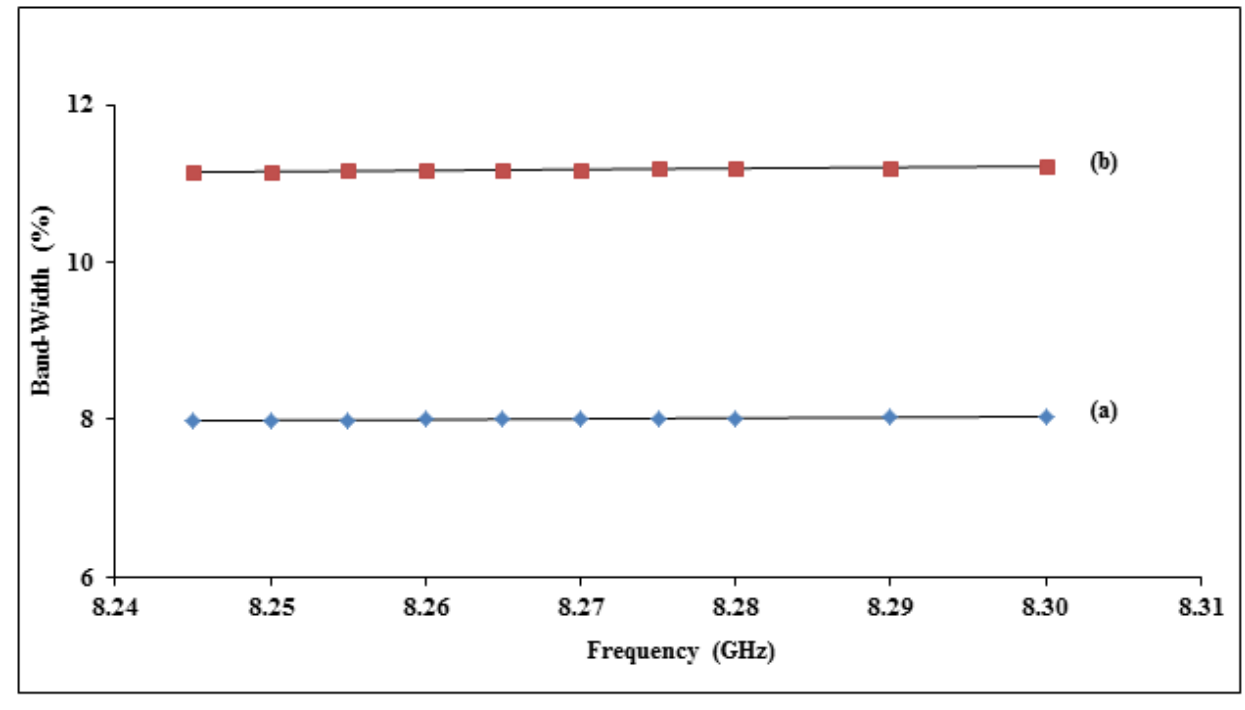


Figure 8: Variation of band width with resonant frequency for (a) unloaded and (b) Gunn loaded ARMSA at a constant threshold voltage of 2.9 V.

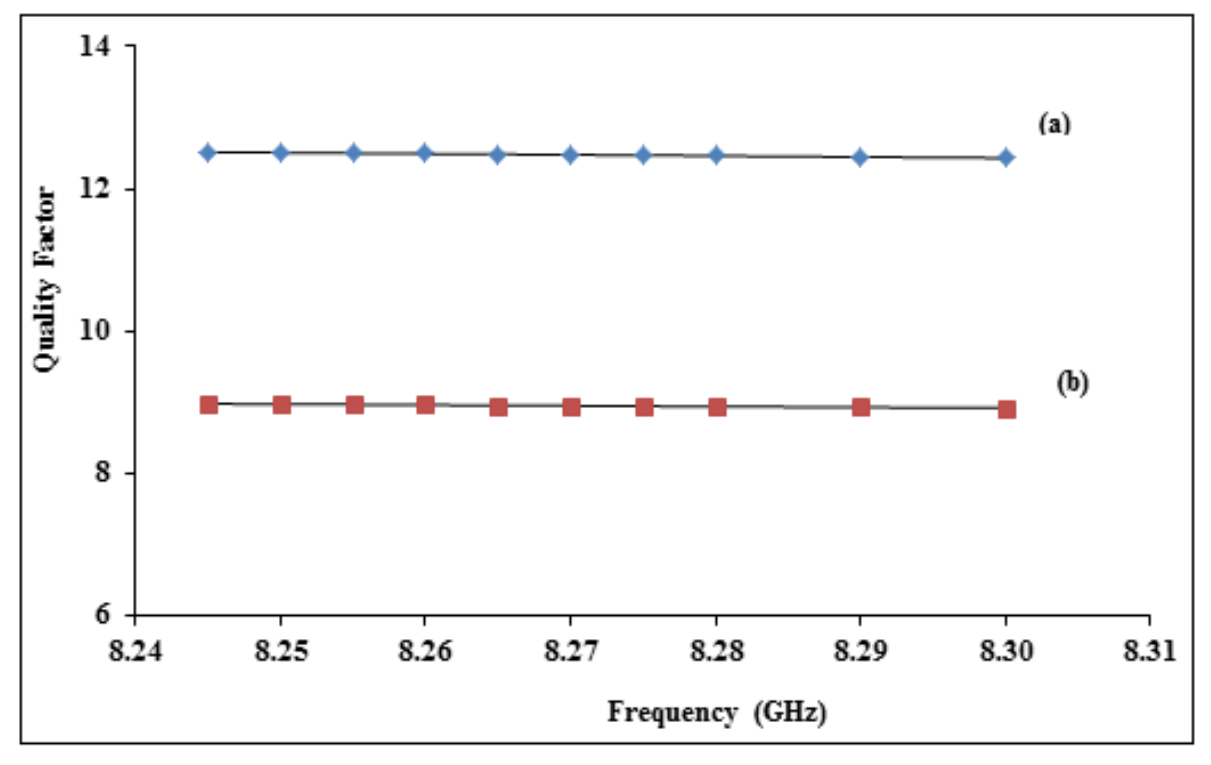


Figure 9: Variation of quality factor with resonant frequency for (a) unloaded and (b) Gunn loaded ARMSA at a constant threshold voltage of 2.9 V.

Vol. No.6, Issue No. 06, June 2017 www.ijarse.com



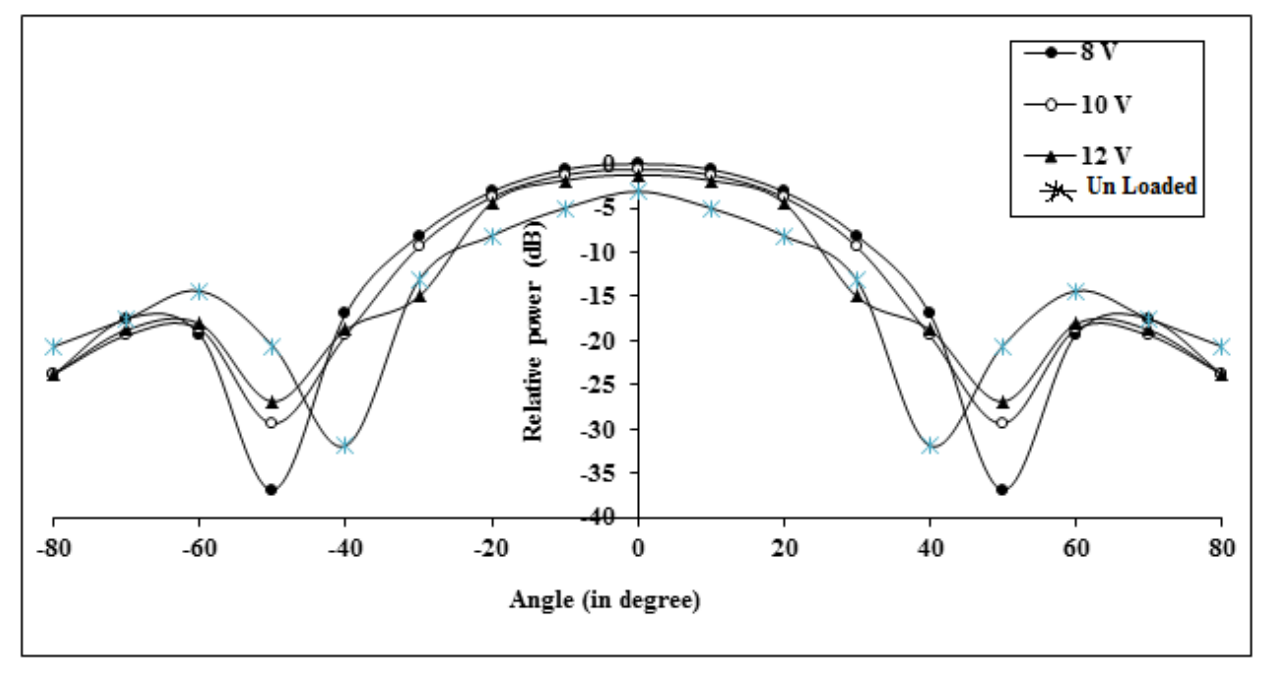


Figure 10: Variation of E-plane radiated power with angle at different bias voltages for unloaded and Gunn loaded